Molecular Cell, Vol. 17, 277–290, January 21, 2005, Copyright ©2005 by Elsevier Inc. DOI 10.1016/j.molcel.2004.12.019

Formation of a Dynamic Kinetochore-Microtubule Interface through Assembly of the Dam1 Ring Complex

Stefan Westermann,[2] Agustin Avila-Sakar,[3] Hong-Wei Wang,[3] Hanspeter Niederstrasser,[2,4] Jonathan Wong,[2] David G. Drubin,[2] Eva Nogales,[1,2,3] and Georjana Barnes[2,*]

[1]Howard Hughes Medical Institute
[2]Department of Molecular and Cell Biology
[3]Lawrence Berkeley National Laboratory
University of California, Berkeley
Berkeley, California 94720

Summary

How kinetochore proteins form a dynamic interface with microtubules is largely unknown. In budding yeast, the 10-protein Dam1 complex is an Aurora kinase target that plays essential roles maintaining the integrity of the mitotic spindle and regulating interactions with the kinetochore. Here, we investigated the biochemical properties of purified Dam1 complex. The complex oligomerized into rings around microtubules. Ring formation was facilitated by microtubules but could occur in their absence. Mutant alleles led to partially assembled complexes or reduced microtubule binding. The interaction between rings and microtubules is mediated by the C termini of both Dam1 and αβ-tubulin. Ring formation promotes microtubule assembly, stabilizes against disassembly, and promotes bundling. A GTP-tubulin lattice is the preferred binding partner for the complex, and Dam1 rings can exhibit lateral mobility on microtubules. These observations suggest a mechanism by which the kinetochore can recognize and stay attached to the plus ends of microtubules.

Introduction

The inheritance of genetic material depends on the faithful segregation of chromosomes during mitosis. The physical connection between centromeres and microtubules is formed by the kinetochore, a complex structure that consists of more than 60 proteins in budding yeast (Cheeseman et al., 2002a; McAinsh et al., 2003). Biochemical characterizations of kinetochore proteins have allowed them to be grouped into distinct subcomplexes (Cheeseman et al., 2002b; De Wulf et al., 2003; Westermann et al., 2003). The organization of these subcomplexes and their interdependencies in associating with centromeric DNA seem to be widely conserved from budding yeast to higher animals (De Wulf et al., 2003; Westermann et al., 2003; Wieland et al., 2004), allowing the investigation of broadly applicable features of kinetochore biology in a genetically tractable organism.

A particularly important, albeit poorly understood, role is played by the microtubule binding proteins of the outer kinetochore. Kinetochores must attach to the spindle with high fidelity to avoid chromosome gain or loss. Importantly, this attachment must be maintained even though the kinetochore microtubules are highly dynamic (Maiato et al., 2004; Pearson et al., 2004). During growth and shrinkage of kinetochore microtubules, the attached chromosomes move vigorously back and forth, thus undergoing "directional instability." How the kinetochore recognizes the plus end of a microtubule, allows the exchange of subunits while maintaining attachment, and mechanically couples the depolymerization of kinetochore microtubules to the generation of force necessary for chromosome movement are fundamental unanswered questions in kinetochore biology.

Detailed molecular analysis of chromosome segregation in budding yeast suggested an important role for nonmotor microtubule-associated proteins (MAPs) in chromosome segregation (He et al., 2001). Among these MAPs are Stu2p, Bim1p, and Bik1p, the budding yeast homologs of XMAP215, EB1, and CLIP-170, respectively. Stu2p is essential for the dynamics of kinetochore microtubules (Kosco et al., 2001; Pearson et al., 2003), as loss-of-function mutants lead to a reduction in the transient separation of sister chromatids (He et al., 2001). Recent biochemical evidence suggests that Stu2p can directly target and destabilize the plus end of a microtubule (van Breugel et al., 2003). The biochemical activities of other microtubule binding proteins at the kinetochore are less well defined. Of special importance for budding yeast spindle function is the Dam1 complex. Dam1p and Duo1p have been identified as essential proteins for mitotic spindle function (Hofmann et al., 1998). Temperature-sensitive mutations in both proteins show two general classes of phenotypes. The first class is defined by broken-down, disorganized or collapsed spindles and suggests an important function in assembly and maintenance of the mitotic spindle (Cheeseman et al., 2001a; Hofmann et al., 1998; Jones et al., 1999). The second class of mutant phenotypes show massive defects in chromosome segregation (Cheeseman et al., 2001a; Janke et al., 2002; Jones et al., 2001). After the initial characterization of Dam1p and Duo1p, additional subunits of the complex were identified by two-hybrid screens (Enquist-Newman et al., 2001) or affinity purifications (Cheeseman et al., 2001b, 2002b; De Wulf et al., 2003; Janke et al., 2002; Li et al., 2002), bringing the total number of subunits to ten. Importantly, the complex has been recognized as a key target of the yeast Aurora kinase Ipl1p in regulating kinetochore-microtubule attachments. Mutations that prevent Ipl1p phosphorylation of Dam1p mimic the phenotype of Ipl1 temperature-sensitive alleles. Conversely, *dam1* mutations that mimic constitutive Ipl1 phosphorylation are able to partially suppress an Ipl1 temperature-sensitive allele (Cheeseman et al., 2002b), demonstrating the importance of Dam1p in the regulation of the microtubule-kinetochore interface in vivo.

The low amount of functional Dam1 complex that can be purified from yeast cells and the fact that individual

*Correspondence: gbarnes@socrates.berkeley.edu
[4]Present address: Department of Cell Biology and Physiology, Washington University School of Medicine, St. Louis, Missouri 63110.

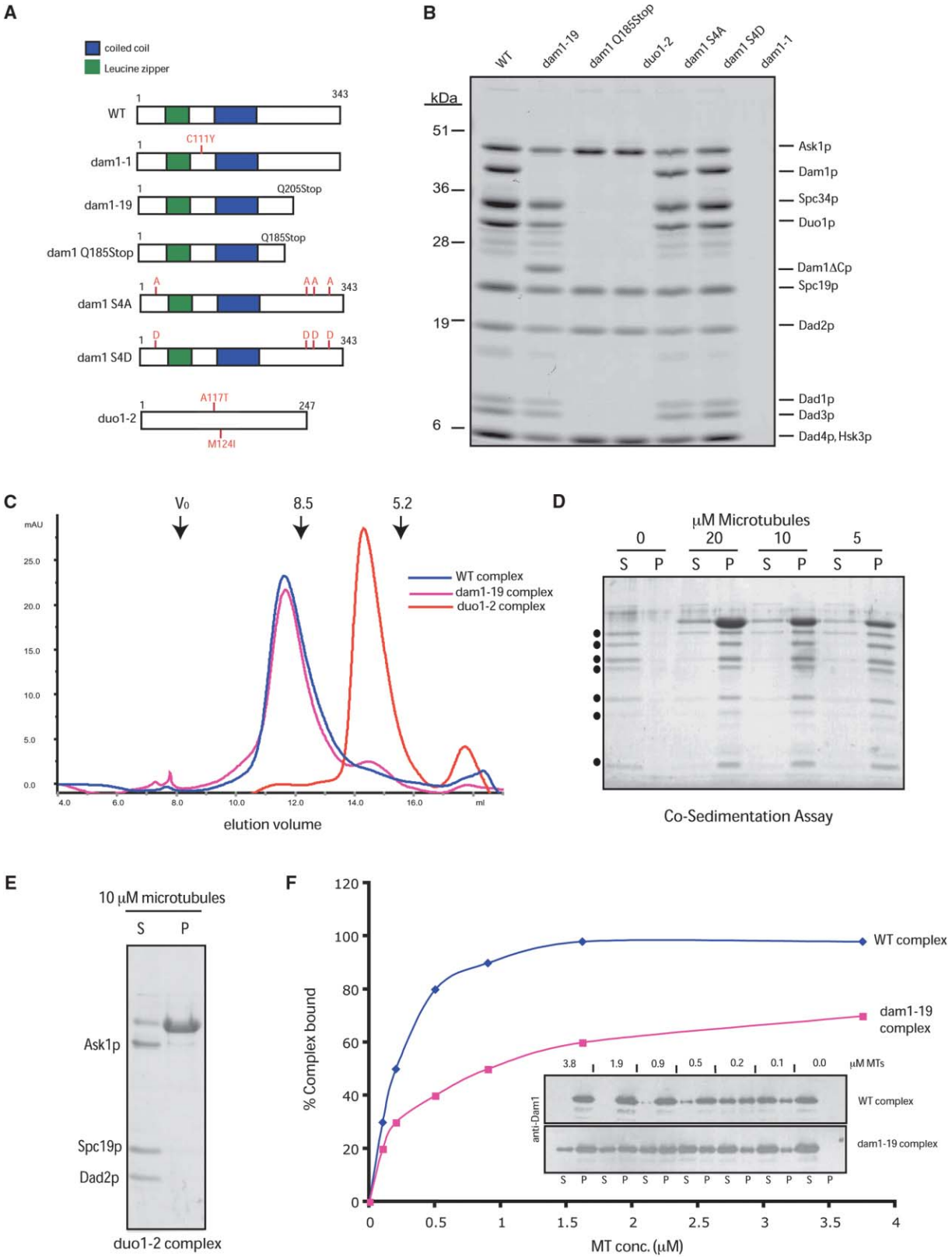

Figure 1. Expression and Characterization of Wild-Type and Mutant Dam1 Complexes

(A) Schematic representation of the mutations introduced into Dam1 and Duo1.

(B) Coomassie-stained 13.5% gel of the purified complexes showing their respective subunit compositions.

(C) Size-exclusion chromatography of Dam1 wild-type (wt), *dam1-19*, and *duo1-2* complexes on a Superose 6 column. Void volume and elution volumes of standard proteins (Thyroglobulin, Stokes Radius 8.5 nm, Catalase, Stokes Radius 5.2 nm) are given at the top.

subunits are insoluble when expressed in bacteria have so far precluded an investigation of the biochemical functions of the Dam1 complex. Here, we use purified, reconstituted Dam1 complex to investigate the structure and function of the complex on microtubules in vitro. Our analysis provides a biochemical explanation for the important roles of this complex in vivo, sheds light on the structural nature of the kinetochore-microtubule interface, and explains important features essential for kinetochore biology in general.

Results

Expression and Purification of Wild-Type and Mutant Dam1 Complexes Reveals Differences in Subunit Composition and Microtubule Binding

To investigate the biochemical activities of the Dam1 complex, we used an expression plasmid that coexpresses all ten subunits of the complex in *E. coli* (Miranda et al., 2005). In addition to the wild-type (wt) complex, we sought to investigate the effect of certain selected mutations on complex function. These mutant complexes corresponded to temperature-sensitive alleles or to *dam1* mutants that either prevent (*dam1* S4A) or mimic (*dam1* S4D) constitutive Ipl1p phosphorylation. The mutants were generated by introducing the corresponding point mutations into the gene on the expression plasmid (Figure 1A). The complexes were purified by nickel-affinity chromatography using a 6× histidine tag fused to the C terminus of the Hsk3p subunit. Conventional chromatography by cation exchange and size exclusion were then used to purify the complexes to apparent homogenity (Figure 1B). The yield was approximately 1 mg of purified complex per liter bacterial culture. The wt complex contained all ten subunits in equal stoichiometry and eluted in size exclusion chromatography as a single species with a Stokes radius of ~97 Å (Figure 1C). Density gradient centrifugation on a 5%–40% sucrose gradient (data not shown) yielded a sedimentation constant of 10.2 S, corresponding to a calculated native molecular weight of ~390 kDa, which is most consistent with the conclusion that the species purified under these conditions is a dimer (2 × 218 kDa) consisting of two heterodecamers.

The *dam1-19* allele lacks the C terminus of Dam1p. The mutant is characterized by slow growth at all temperatures and collapsed mitotic spindles at the restrictive temperature of 37°C (Cheeseman et al., 2001a). The purified dam1-19 complex contained all ten subunits (Figure 1B) and eluted close to the position of the wt complex during gel filtration (Figure 1C), demonstrating that the C-terminal 138 amino acids of Dam1p are dispensable for complex formation. In contrast, further truncation of the Dam1p C terminus by 20 amino acids to generate *dam1Q185Stop* yielded a partially assembled complex that, when expressed at 37°C and purified under identical conditions, consisted only of the five subunits Ask1p, Spc19p, Dad2p, Dad4p, and Hsk3p. As evidenced by gel filtration, these subunits formed a stable complex with a Stokes radius of 60 Å (Figure 1C), whereas the remaining subunits remained insoluble in the pellet fraction of the purification. The same partially assembled complex was purified when the complex contained the *duo1-2* mutation. In contrast, complexes expressing the Ipl1p phosphorylation-site mutants retained full assembly of all subunits (Figure 1B). We were unable to purify a soluble complex with the *dam1-1* mutation, even when trying various expression conditions. This might suggest that the mutated residue cysteine 111 could participate in intra- or intermolecular disulfide bonds that might be necessary for complex formation.

Microtubule Binding of Wt and Mutant Complexes

To analyze microtubule binding, limited amounts of the complexes were incubated with taxol-stabilized bovine brain microtubules and centrifuged, and supernatant and pellet fractions were analyzed by SDS-PAGE. As shown in Figure 1D, the entire Dam1 complex binds to microtubules with high affinity. In contrast, the partially assembled *duo1-2* complex is found in the supernatant of the cosedimentation assay, demonstrating that it is unable to interact with microtubules (Figure 1E). To analyze more subtle differences in binding affinities, we varied the microtubule concentration over the range of 0–3.8 μM in a cosedimentation experiment. Binding was followed by Western blotting with an anti-Dam1p antibody. The binding of wt complex to microtubules was concentration dependent and saturable, with an apparent dissociation constant of K_D ~0.2 μM (Figure 1F). In contrast, the *dam1-19* complex showed much weaker binding, with a dissociation constant of K_D ~0.8 μM, whereas maximally only 70% of the mutant complex was bound to microtubules. Thus, the C-terminal domain of Dam1p is dispensable for complex formation but is required for optimal microtubule binding. We did not observe noticeable differences in the binding affinities of the phosphomutants *dam1S4A* and *dam1S4D* of the Ipl1 sites compared to wt complex (data not shown). Consistent with these results, in vitro phosphorylation of recombinant Dam1 complex with bacterially expressed Ipl1p kinase did not significantly change the microtubule binding properties of the complex (data not shown).

Formation of the Dam1 Ring Complex

To visualize Dam1 complex bound to microtubules, aliquots of the binding reactions were analyzed by negative stain electron microscopy. At substoichiometric ratios of Dam1 complex to microtubules, prominent rings that completely encircled the microtubule orthogonal to its axis were readily observed (Figure 2A). Ring formation was also observed by using native Dam1 complex iso-

(D) Coomassie-stained gel of microtubule binding assay of wt complex. S and P denote supernatant and pellet fraction, respectively.
(E) Microtubule binding assay of partially assembled *duo1-2* complex.
(F) Determination of binding affinities for wt and *dam1-19* complexes to microtubules by cosedimentation assay. Dam1 in supernatant (S) and pellet (P) fractions was followed by Western blotting with an anti-Dam1 antibody. Binding was quantified and expressed as a percentage of complex found in the pellet fraction.

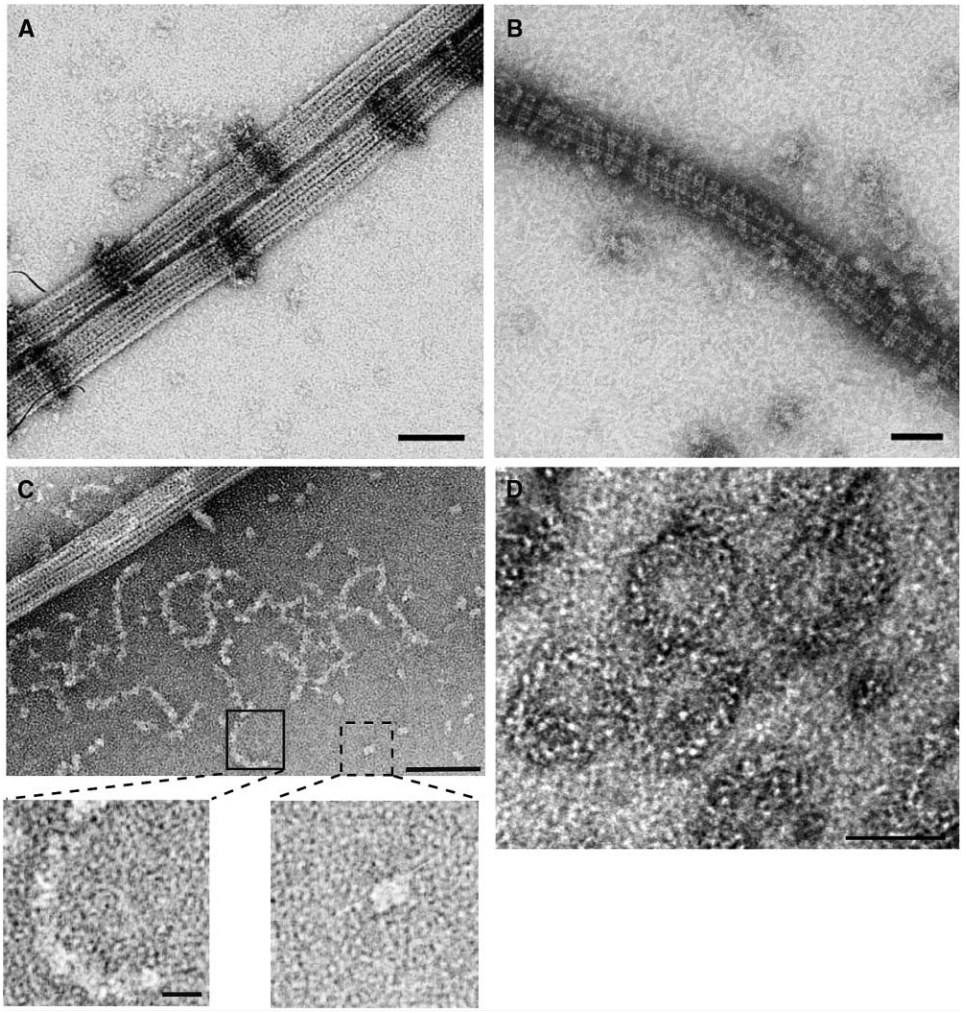

Figure 2. Electron Microscopy Reveals Decoration, Composition, and Self-Assembly of the Dam1 Ring Complex

(A) Purified Dam1 complex was bound to taxol-stabilized bovine brain microtubules and visualized by electron microscopy (EM) by using negative stain. Bar, 50 nm.

(B) At higher concentrations of Dam1 complex, complete decoration is observed.

(C) Microtubule binding reactions were diluted prior to EM and visualized with negative stain. Dam1 rings in various states of disassembly can be seen in the vicinity of the microtubule. Dashed box shows smallest subunit corresponding to the basic building block of the ring. Solid box shows half ring assembled by longitudinal association of the small building blocks. Bar, 10 nm.

(D) Pure Dam1 complex at 0.2 mg/ml was incubated on a phospholipid monolayer for 48 hr and visualized by EM using negative stain. Self-assembled Dam1 rings are visible. Bar, 40 nm.

lated directly from yeast cells, the *dam1* phosphomutants, and the *dam1-19* complex (data not shown).

With saturating amounts of complex, complete decoration of microtubules could be seen (Figure 2B). Without additional systematic image analysis of well-ordered assemblies, it is not absolutely clear whether at these higher concentrations Dam1 complex is forming rings that are closely stacked or a continuous helical filament (or both). We were able to reveal apparent Dam1 ring disassembly intermediates in the vicinity of microtubules by diluting the binding reactions 1000-fold prior to electron microscopy (EM) (Figure 2C). These apparent disassembly products suggest a possible mode of ring subunit organization. The smallest structures visible were fairly regular in size and shape (Figure 2C, dashed box) with a length of about 105 Å and a diameter of about 70 Å. This size is not compatible with tubulin subunits, instead the width is the same as observed in fragmented rings of the complex seen in the vicinity (Figure 2C, solid box). Thus, these subunits are likely the basic building block of the ring and associate longitudinally to form rings around microtubules.

The observation of Dam1 ring assembly raised the question of whether these structures would only form in the presence of microtubules. In the absence of microtubules, Dam1 preparations showed a few small, curved aggregates, reminiscent of the disassembly product shown in Figure 2C. However, when the protein was bound to lipid monolayers during 2D-crystallization attempts, both fragments and full rings were readily observed (Figure 2D). Rings formed under these conditions were fairly regular in size but somewhat smaller than

those associated with microtubules (see below), with an outer diameter of about 450 Å and an inner diameter of about 290 Å. Ring assembly was also observed when Ni bound NTA-lipids (that interacted with the His-tag) or negatively charged phospholipids were used, suggesting that ring assembly is likely the result of concentrating the Dam1 complex on a surface.

Cryo-EM of GMPCPP Microtubules Decorated with Dam1 Complex

To analyze the decoration of microtubules with Dam1 complex under native conditions, we used cryo-EM of frozen hydrated samples in vitreous ice. We tested two types of stabilized microtubule substrates for this analysis: taxol-stabilized bovine brain microtubules and microtubules assembled in the presence of the slowly hydrolyzable GTP analog GMPCPP (Guanosine-5′-[(α,β)-methyleno]triphosphate). Previous studies have demonstrated that these microtubules differ in average number of protofilaments and the precise axial repeat of tubulin monomers along the protofilament (Hyman et al., 1995).

We noticed that the decoration of GMPCPP microtubules was more uniform and that the Dam1 rings appeared more ordered, with long stretches of microtubules showing regular ring spacing and dimensions compared to the decoration of taxol-stabilized microtubules (data not shown). We therefore used GMPCPP microtubules decorated with Dam1 complex to calculate the dimensions and spacing of the rings. We analyzed the diffraction pattern of selected stretches of decorated microtubules (Figure 3A). The Fourier transformation (Figure 3B) revealed layer lines at 43 and 21 Å, corresponding to the microtubule lattice (white arrows), and an additional, broader layer line corresponding to the axial repeat of the bound rings around the microtubule at about 100 Å (white arrowheads). A filtered image generated with these three layer lines plus the equator is shown in Figure 3C. The density profile obtained by integrating this filtered image along the microtubule axis is shown beneath. From the major peaks in the density profile we estimate the outer diameter of the rings to be about 540 Å and the inner diameter to be 320 Å.

Complex Binding and Ring Formation Depends on the Presence of the C Terminus of αβ-Tubulin

The wrapping of the Dam1 rings around the microtubule strongly suggested an involvement of the C-terminal tails of α− and β-tubulin in its interaction with the microtubule. To test this possibility, we analyzed the decoration of subtilisin-digested or control microtubules by cryo-EM. Extended subtilisin digest resulted in the release of the C termini of both α- and β-tubulin (Figure 4A). Complete digestion was confirmed by Western blotting with a β-tubulin antibody whose epitope is located in the C-terminal domain (data not shown). Control microtubules showed strong decoration by the Dam1 ring complex, whereas only bare microtubules were found in the subtilisin-digested sample (Figure 4B). Upon shorter digests, which only removed the C terminus of β-tubulin, we still observed significant ring formation (data not shown).

To further analyze binding of the Dam1 complex to microtubules, we covalently linked the fluorescent dye Alexa-488 to recombinant Dam1 complex. Labeled complex and nonincorporated dye were separated by gel filtration. Analysis of the Coomassie-stained gel of this preparation by UV illumination revealed that the label was incorporated into the Spc34p and Spc19p subunits of the Dam1 complex (Figure 4C). Microtubule binding assays and analysis by EM demonstrated that the Alexa-488-Dam1 complex formed normal rings around microtubules (Supplemental Figure S1 available online at http://www.molecule.org/cgi/content/full/17/2/277/DC1) and bound to microtubules with comparable affinity to wt complex. We digested taxol-stabilized, rhodamine microtubules with the protease subtilisin to remove the C termini of α- and β-tubulin and tested binding of Alexa-labeled Dam1 complex to the microtubules by fluorescence microscopy. Control microtubules showed robust binding of fluorescently-labeled Dam1 complex (Figures 4D and 4F). Microtubules decorated with the complex were often organized into thick bundles (see below). In contrast, subtilisin-digested microtubules showed little, if any, decoration with the labeled complex (Figures 4E and 4G). We conclude that complete removal of the C termini of α- and β-tubulin prevents Dam1 complex binding and formation of the Dam1 ring complex on microtubules.

The Dam1 Ring Complex Promotes Tubulin Polymerization and Microtubule Stability In Vitro

The Dam1 complex has an important role in spindle integrity in vivo, as temperature-sensitive mutants of its subunits are unable to assemble or maintain a normal mitotic spindle. We therefore investigated the effects of the Dam1 complex on microtubule assembly in vitro.

Polymerization of pure brain tubulin into microtubules was followed by an increase in light scattering at 350 nm. Under our conditions, 10 μM tubulin (1 mg/ml) alone did not assemble into microtubules over the course of the experiment. However, addition of Dam1 complex in substoichiometric amounts led to a rapid, concentration-dependent increase in light scattering (Figure 5A). To confirm that this increase was due to the formation of microtubules, an aliquot of the reaction was fixed with glutaraldehyde and centrifuged onto coverslips, and the microtubules were visualized by immunofluorescence with a tubulin antibody. This analysis confirmed the formation of numerous microtubules in the presence of Dam1 complex, but not in the control reaction (Figure 5B).

A complex that forms a ring around a microtubule might increase the stability of the polymer. We tested this possibility by assembling microtubules from 15 μM tubulin in the presence and absence of Dam1 complex. These microtubules were then rapidly diluted, and their disassembly was followed by light scattering and by a sedimentation assay. Figure 5C demonstrates that control microtubules rapidly depolymerized when they were diluted below the critical concentration and that the bulk of tubulin was found in the supernatant after centrifugation (Figure 5D). In contrast, microtubules assembled in the presence of Dam1 complex depolymerized more slowly, retained a higher light scattering signal, and had more tubulin in the pellet of the centrifugation. Thus, the Dam1 complex promotes microtubule

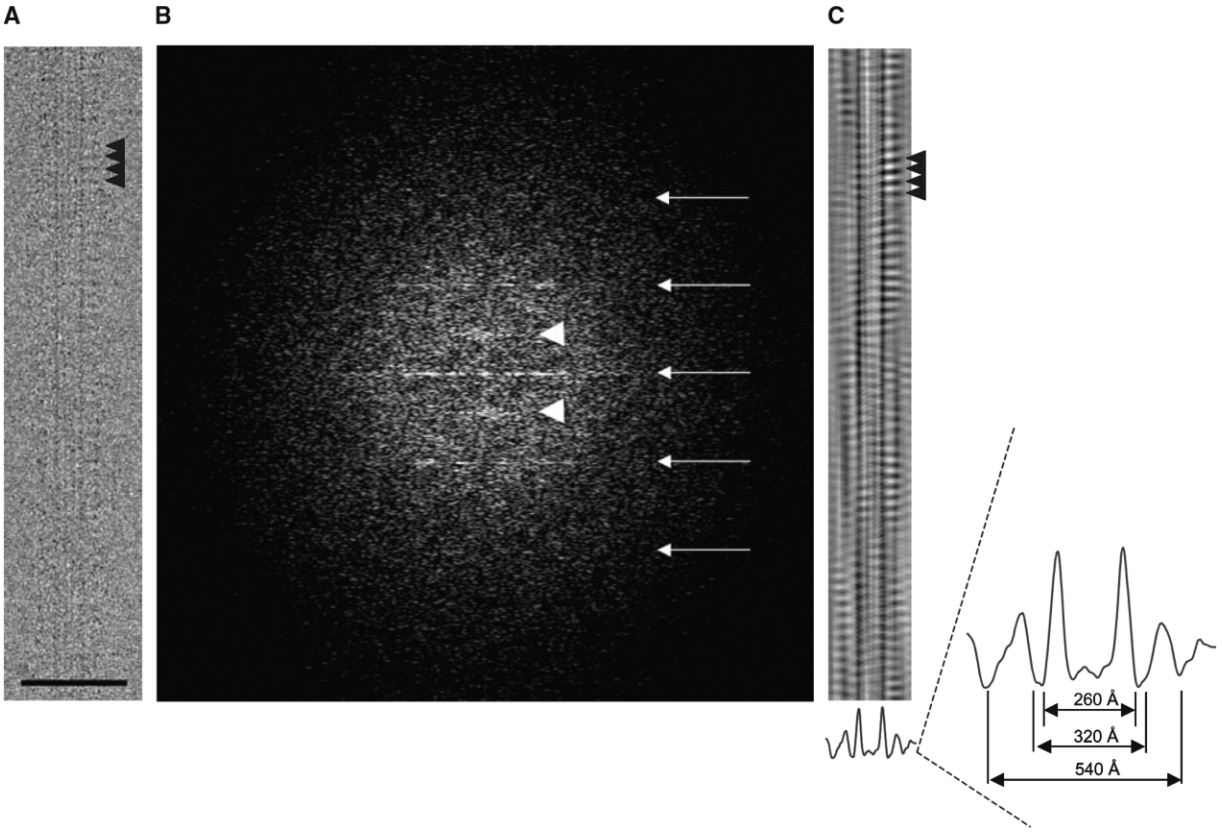

Figure 3. Analysis of Dam1 Ring Decoration on GMPCPP Microtubules by Cryo-EM

(A) Analysis of Dam1 decoration. Cryo-EM micrograph of Dam1 decorated microtubule. Black arrowheads point to adjacent Dam1 rings.
(B) Fourier transform of microtubule as shown in (A). White arrows point to a series of horizontal lines (43 and 21 Å layer lines) generated by diffraction of the microtubule. White arrowheads point to the layer line at 100 Å generated by diffraction from the Dam1 complex.
(C) Computer-filtered image of the analyzed microtubule. Density profile of the filtered image across the microtubule and estimation of the dimensions of the Dam1 ring complex. Bars, 100 nm.

assembly and stabilizes microtubules against dilution-induced disassembly.

The Dam1 Ring Complex Organizes Microtubules into Long Bundles In Vitro

Next, we investigated the effects of the Dam1 complex on the assembly of higher concentrations of tubulin. In our assembly assay, 15 μM tubulin showed a slow increase in light scattering with an extended lag period (Figure 5E). Increasing the amount of Dam1 complex increased the rate of tubulin assembly and reduced the lag period. Importantly, fixed aliquots of the assembly reactions that were sedimented onto coverslips and stained with an anti-tubulin antibody revealed distinct microtubule morphologies: whereas the control reactions displayed single microtubules with an average length of 10–15 μm (Figure 5F), microtubules assembled in the presence of the Dam1 complex were frequently organized into long bundles (Figure 5G) with an average length of 35–45 μm. Analysis of these microtubules by EM revealed the presence of bundles of typically four to six microtubules that were decorated to varying degrees with Dam1 rings (Figure 5I). Sometimes rings on adjacent microtubules showed direct lateral contacts (Figure 5I insert), suggesting that bundling could be aided by direct ring-to-ring interactions.

Binding of Alexa 488-Labeled Dam1 Ring Complex to Various Microtubule Substrates: Preference for a GTP Lattice

We used Alexa-labeled Dam1 complex to analyze further aspects of its binding to various microtubule substrates. When rhodamine-labeled GMPCPP microtubules were incubated with limiting amounts of Alexa-Dam1 complex and then visualized by fluorescence microscopy, a striking punctate decoration of microtubules was observed (Figures 6A and 6B). Accordingly, a line scan of the Alexa signal along a single GMPCPP microtubule revealed discrete signals that often displayed the same intensity (Figure 6C). As the same binding conditions revealed single ring decoration by EM, the fluorescent signals likely corresponded to individual rings.

To fulfill their function, kinetochores must associate with and remain attached to microtubule ends. Kinetochore proteins assembled on beads coated with centromeric DNA in vitro can preferentially bind to the GTP lattice of a microtubule (Severin et al., 1997). However, which subunits of the kinetochore are responsible for

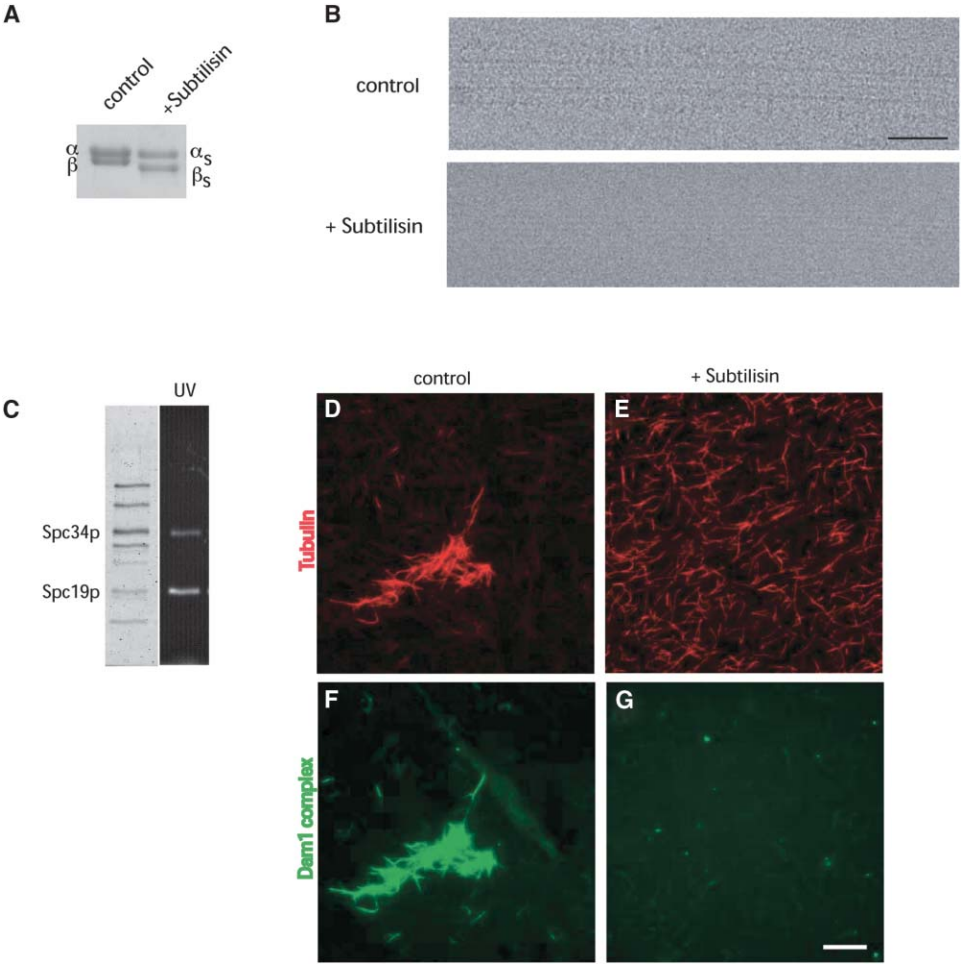

Figure 4. Dam1 Complex Binding and Ring Formation Depend on the α- and β-Tubulin C Termini

(A) Taxol-stabilized bovine brain microtubules were digested with subtilisin. Coomassie-stained gel (containing 6 M urea to enhance separation of α- and β-tubulin) of the digest showing shift of α- and β-tubulin mobility.

(B) Cryo-EM analysis of Dam1 complex binding to subtilisin-digested microtubules. Control microtubules show normal decoration (top), whereas only bare microtubules are observed in the protease treated preparation (bottom). Bar, 50 nm.

(C) Preparation of Alexa-labeled Dam1 complex. Coomassie-stained gel of preparation is on the left. UV illumination of the gel reveals covalent labeling of the Spc34 and Spc19 subunits of the Dam1 complex by the dye.

(D) Rhodamine-labeled control microtubules (red) bind Alexa488-labeled Dam1 complex (green) and get bundled (F), whereas subtilisin-digested microtubules (E) do not (G). Bar, 10 μm.

this important feature is not known. As GMPCPP microtubules, which mimic the GTP lattice of a microtubule, seemed to be the preferred substrate for Dam1 decoration in our cryo-EM analysis, we sought to analyze further whether the Dam1 ring complex showed a preference for this type of lattice over a GDP lattice. For this experiment, we prepared segmented microtubules that consisted of an unlabeled GMPCPP seed that was elongated by using rhodamine-labeled GTP-tubulin. After incorporation into the lattice, the GTP is rapidly hydrolyzed, thus producing segmented microtubules consisting of an unlabeled GMPCPP segment and two labeled GDP segments. The segmented microtubules were mixed with limiting amounts of Alexa-labeled Dam1 complex, fixed, and visualized by fluorescence microscopy. Strikingly, a stronger decoration of the segmented microtubules with Alexa488-Dam1 complex was found on the GMPCPP parts of the lattice (Figures 6D and 6E). The corresponding intensity scan further revealed this distribution of the complex (Figure 6F). We quantified the decoration by counting clearly segmented microtubules in randomly chosen fields and ordered them into three categories (Figure 6G); more than 50% ($n = 100$) of the segmented microtubules showed a strong decoration of the GMPCPP segment and one end of the microtubule (Figure 6G). In most cases (~80%), this end decoration was on the longer rhodamine segment, suggesting that it corresponds to the plus end of the microtubule. In about 35% of the microtubules, the strong decoration of just the GMPCPP segment was apparent, whereas only 12% of microtubules displayed evenly distributed Dam1 rings. The preferred binding to the GMPCPP segement was not due to the lack of a rhodamine label on this part of the lattice, as binding to segmented control microtubules that were completely stabilized with taxol showed no bias for the unlabeled

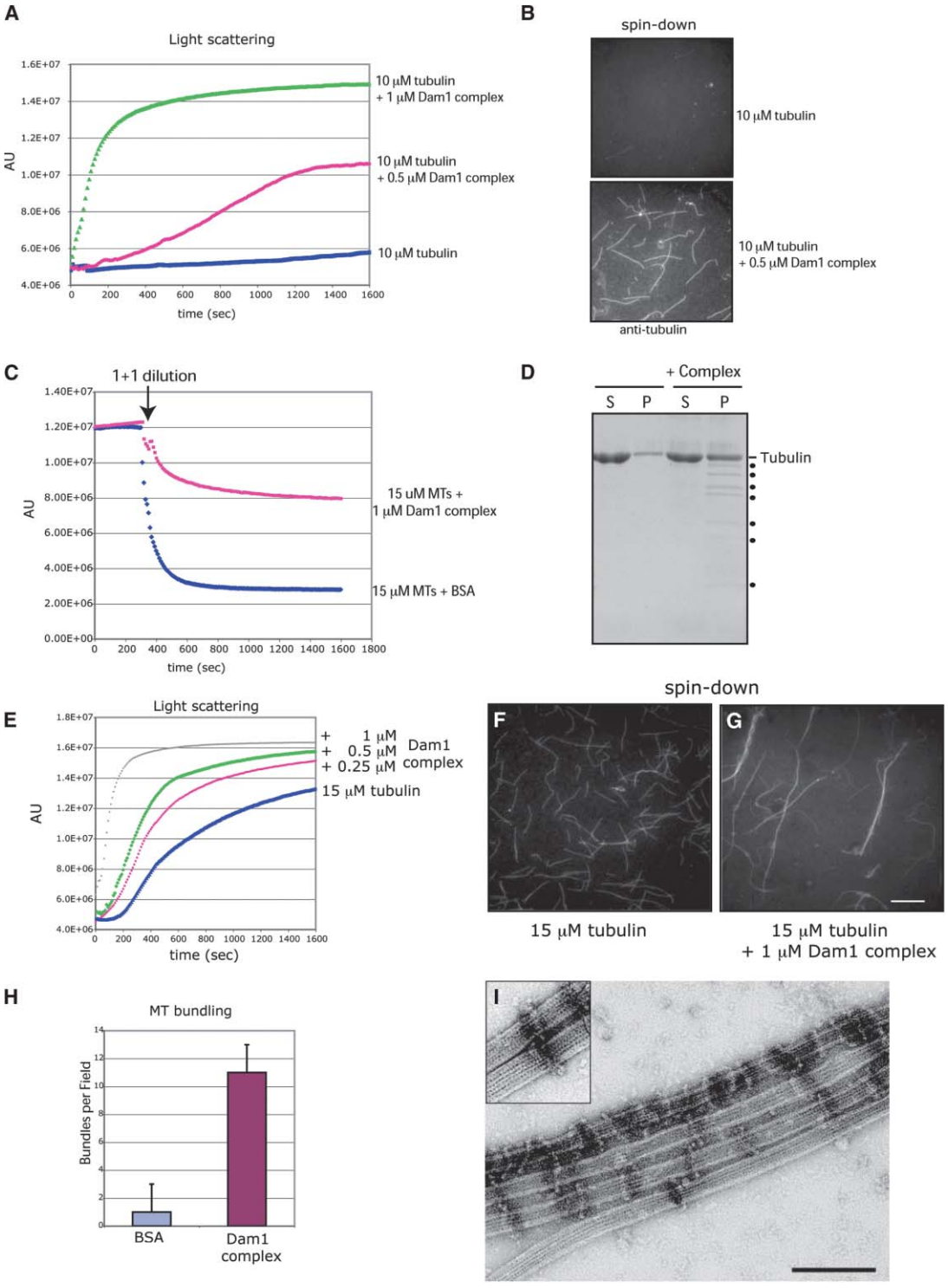

Figure 5. Biochemical Activities of the Dam1 Ring Complex on Microtubules In Vitro

(A) Light-scattering assay of tubulin assembly in the absence and presence of the Dam1 complex. Addition of Dam1 complex increases rate of tubulin assembly.

(B) Reactions from (A) were fixed, centrifuged, and pelleted onto coverslips. Staining with an anti-tubulin antibody demonstrates that microtubules are only formed in the presence of Dam1 complex.

(C) Microtubule stability experiment. Microtubules were assembled from 15 μM tubulin in the presence and absence of Dam1 complex and then rapidly diluted.

(D) Reactions from (C) were centrifuged, supernatants (S) and pellets (P) were separated, run on a 12.5% SDS-PAGE gel, and stained with Coomassie. Black dots indicate subunits of the Dam1 complex.

(E) Assembly of 15 μM tubulin incubated with increasing amounts of Dam1 complex followed by light scattering.

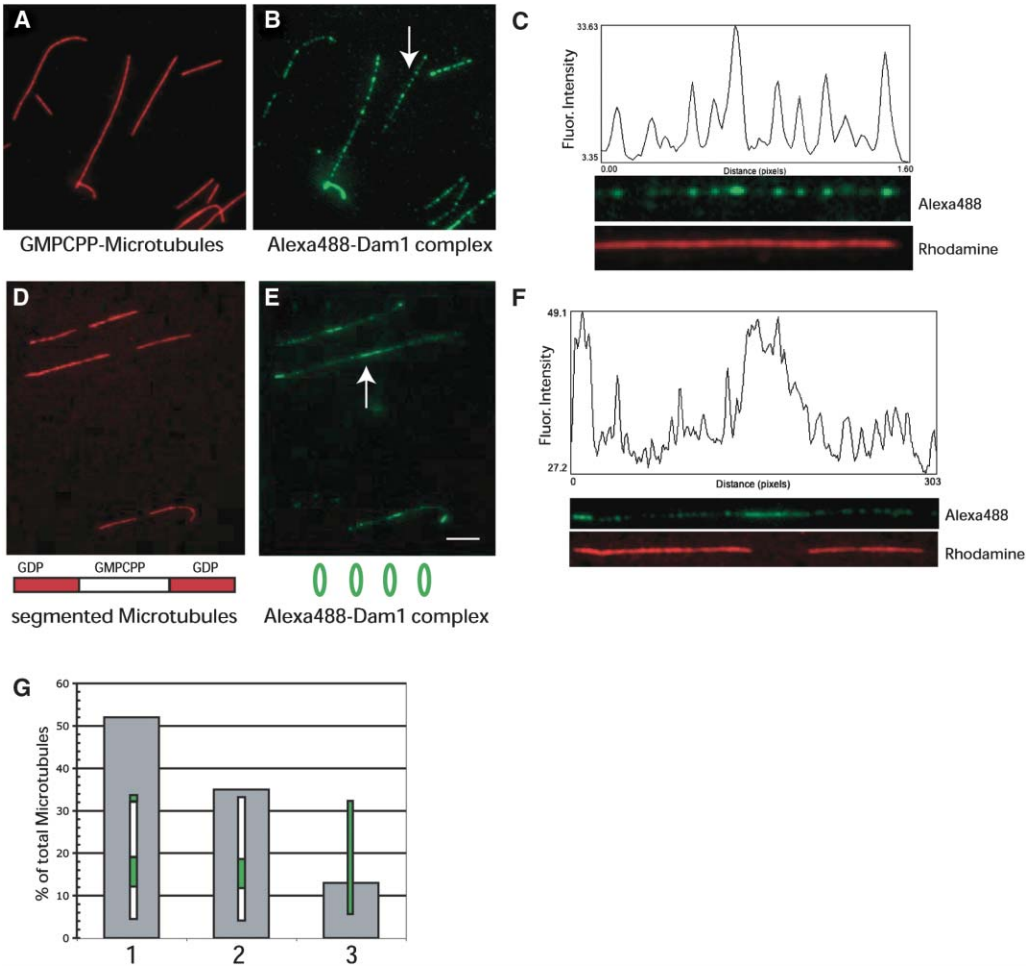

Figure 6. Analysis of Microtubule Binding with the Alexa488-Dam1 Complex

(A) GMPCPP-stabilized, rhodamine microtubules were incubated with limiting amounts of Alexa-Dam1 complex and visualized by fluorescence microscopy.

(B) Note the punctate decoration of microtubules with the Alexa-labeled complex.

(C) Intensity scan of the microtubule reveals discrete signals.

(D) Decoration of segmented GMPCPP/GDP microtubules with Alexa-Dam1 complex. Microtubules are composed of an unlabeled segment assembled with GMPCPP and two rhodamine labeled segments containing GDP-tubulin.

(E) The Alexa-labeled complex preferentially binds to the GMPCPP segments of the microtubules. Bar, 5 μm.

(F) Intensity scan shows stronger decoration on the GMPCPP segment and on one end of the microtubule.

(G) Quantitation of the decoration of segmented microtubules. 100 clearly segmented microtubules in random fields were counted and ordered into three categories: (1) microtubules with a stronger decoration of the GMPCPP segment or one end, (2) microtubules with a stronger decoration only of the GMPCPP segment, and (3) microtubules with an evenly distributed decoration.

segments (data not shown). Thus, the cryo-EM analysis together with the decoration of segmented GTP/GDP microtubules suggest that a GTP lattice is the preferred binding partner for the Dam1 ring complex.

Behavior of the Dam1 Ring Complex on Depolymerizing Microtubules: Evidence for Ring Sliding

During the course of the previous experiments, we noticed that because the GDP segments of the mixed microtubules are not stable, they rapidly disassembled upon dilution. When the distribution of Dam1 rings was analyzed after disassembly of the GDP segments, we noticed that both ends of the remaining GMPCPP segments were strongly labeled for Dam1 rings, suggesting that during microtubule disassembly, rings remained attached to the shortening microtubules (data not shown). We wanted to analyze this behavior of the Dam1 ring complex in a more controlled manner. GMPCPP microtubules were loaded with limiting amounts of Dam1

(F) Control reaction from (E) centrifuged onto coverslips and stained with a tubulin antibody.

(G) Assembly in the presence of Dam1 complex leads to the formation of long bundles of microtubules. Bar, 10 μm.

(H) Quantitation of bundling activity. Clearly recognizable bundles in randomly chosen fields were counted and compared to a control.

(I) Bundling visualized by EM using negative stain. Insert shows rings on adjacent microtubules directly contacting each other. Bar, 100 nm.

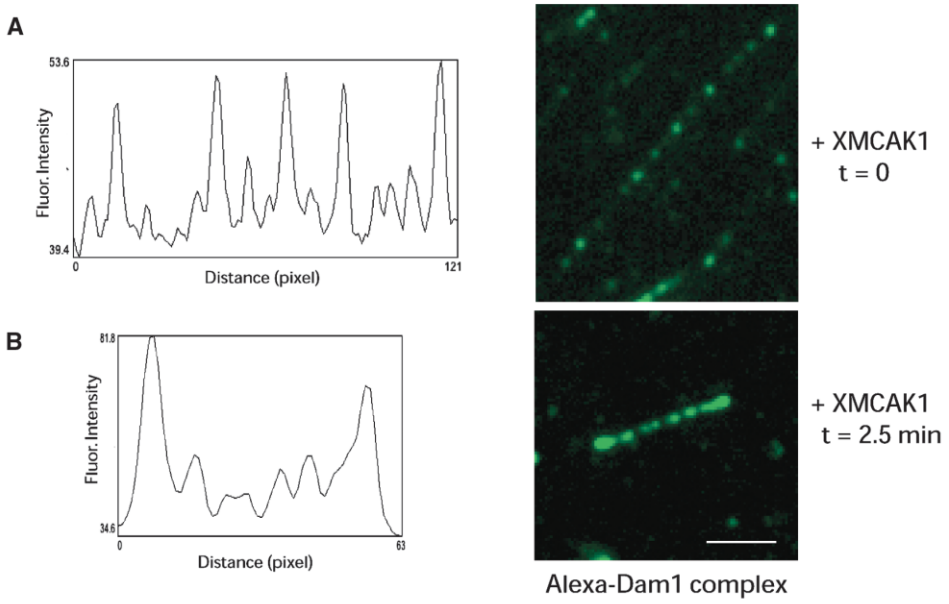

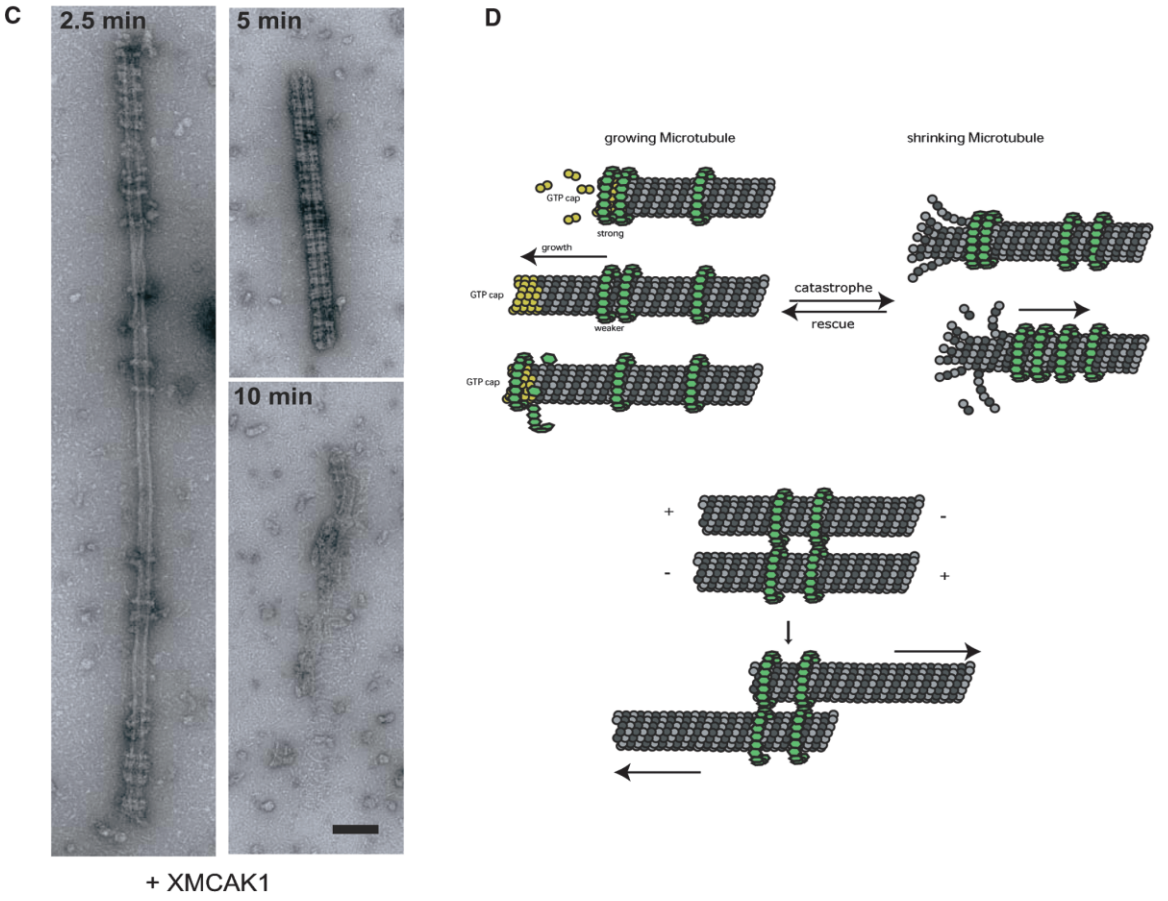

Figure 7. Dynamic Behavior of the Dam1 Ring Complex on Depolymerizing Microtubules

(A and B) Distribution of Alexa-labeled Dam1 complex (green) on GMPCPP microtubules before and after depolymerization induced by XMCAK1. Microtubules were incubated with limiting amounts of Alexa-labeled complex. At t = 0 microtubules show weak punctate decoration with no preference for ends (A). After incubation with the depolymerizing kinesin XKCM1, only short microtubules with brightly-labeled ends are found (B). Bar, 5 μm.

(C) In a parallel experiment, samples were visualized by EM using negative stain. After 2.5 min incubation with XMCAK1, rings accumulate on both ends behind the peeling protofilaments. After 5 min, only very short microtubules that are densely packed with Dam1 rings are found. After 10 min, microtubules disintegrate and release the Dam1 complex. Bar, 50 nm.

rings. To induce disassembly of these microtubules, we added the kinesin XMCAK1, which catalyzes depolymerization by peeling protofilaments from both ends of the microtubules (Desai et al., 1999). The reactions were fixed at various times and visualized by fluorescence microscopy. Figure 7A shows a representative example of the decoration of GMPCPP microtubules at t = 0: a long microtubule is sparsely labeled with Dam1 rings that show no obvious preference for the ends (see also Figure 6B). After 2.5 min incubation with the enzyme, the bulk of microtubules have depolymerized, and the remaining short microtubules show a decoration with a characteristic accumulation of rings on both ends of the microtubules (Figure 7B). Out of 50 short microtubules analyzed after XMCAK1 incubation, 41 showed a strong Alexa signal on both ends (82%). To confirm that the strong Alexa signal indeed corresponded to an accumulation of rings on the ends of depolymerizing microtubules, we performed a parallel experiment in which samples were analyzed by EM using negative stain. Figure 7C shows a representative microtubule after 2.5 min incubation with XMCAK1. The ends of the microtubule show a dense decoration with Dam1 ring complex just behind the peeling protofilaments, corresponding well to the fluorescence image in Figure 7B. After 5 min, only a few short microtubules were visible. These were completely decorated with Dam1 rings along their length. After 10 min, the remaining microtubules disintegrate and release the complex. Taken together, these observations support the conclusion that upon depolymerization of the microtubule, the Dam1 rings do not immediately dissociate or disassemble but remain attached to the microtubule ends and slide back with peeling protofilaments.

Discussion

Assembly of the Dam1 Ring Complex

The rings formed around microtubules by the Dam1 complex are remarkable structures that are clearly not formed by any other microtubule binding protein investigated to date. All other microtubule binding proteins whose association with microtubules has been visualized follow the path of the protofilament and/or bind with the axial repeat of tubulin dimers. One exception is γ-tubulin and its associated proteins in the γ-tubulin ring complex, which form a ring that binds to the microtubule minus end (Zheng et al., 1995). Our studies indicate that the Dam1 rings are formed by longitudinal self-assembly of multiple copies of the Dam1 complex upon the microtubule surface. Although the presence of microtubules strongly facilitates the oligomerization process, ring assembly seems to be an intrinsic property of the Dam1 complex, as we have been able to induce self-assembly into rings in the absence of microtubules. At this point, it is not clear how binding to the lipid monolayer contributes to ring formation. It is likely that the effect is the result of an increase in local concentration of the protein complex as it binds to the monolayer. The microtubule could have a similar effect, interacting with the Dam1 complexes and thus increasing their local concentration at the microtubule surface above the critical concentration for self-assembly. In addition, the negative charge on the C terminus of tubulin could also neutralize the overall positive charge in the Dam1 complexes and thus facilitate their interaction. Indeed, it seems likely that electrostatic interactions play an important role in this process as high-salt conditions prevent oligomerization and microtubule binding, whereas low-salt conditions support them (S.W., D.G.D., and G.B., unpublished data). The behavior of the complex in this regard is very reminiscent of the GTPase dynamin, which self-assembles into rings and helical stacks under low-salt conditions and is thought to form these structures around the necks of invaginated coated pits to support constriction (Hinshaw and Schmid, 1995). Interestingly, dynamin was first purified as a microtubule-associated protein (Shpetner and Vallee, 1989).

Why Form a Ring?

The assembly of ten small proteins into a complex, and the subsequent oligomerization of multiple complexes into a ring, seems to be a very complicated way to construct a microtubule binding structure. However, a microtubule binding ring might be uniquely suited to fulfill the functions of the Dam1 complex within the cell. We demonstrated that the Dam1 ring complex is an excellent microtubule stabilizer and that it strongly promotes microtubule growth through the addition of further subunits. Because the stability of a microtubule is thought to be largely governed by the lateral interactions between adjacent protofilaments (Nogales et al., 1999), rings that bind orthogonal to the microtubule axis are expected to strengthen interprotofilament interactions and additionally to prevent protofilament peeling, which in turn would encourage further growth (Figure 7D, top).

Additional observations identify another potentially significant property of Dam1 ring complexes. We demonstrated that binding between the ring and the microtubule is mediated by flexible domains, involving the C terminus of Dam1p and the C terminus of αβ-tubulin, and is largely electrostatic in nature. These observations open as a possibility the lateral sliding or diffusion of Dam1 rings along microtubules. It should be noted that some single-headed kinesins are thought to move by undirected lateral diffusion along the microtubule and that this type of interaction is also mediated by the flexible C-terminal domains of αβ-tubulin (Okada and

(D) Model for the molecular functions and behaviors of the Dam1 ring complex. Top, preferred binding of the complex to the GTP cap of growing microtubules could stabilize the cap and promote the addition of further tubulin subunits. Lateral diffusion of the rings or de novo assembly can ensure continued association of Dam1 rings with the GTP cap. In case of a catastrophe, peeling protofilaments shorten the microtubule, but the rings do not disassemble but instead slide back on the lattice. Thus, Dam1-associated chromosomes could maintain association with growing and shrinking microtubules. Bottom, lateral mobility of the Dam1 ring complex could allow dynamic bundling of microtubules. Bundling of microtubules with opposite polarity by ring-to-ring interaction could allow motors to move the microtubules against each other while maintaining integrity of the bundle. This could be important for spindle elongation during anaphase B.

Hirokawa, 2000). Moreover, we provide evidence for this type of dynamic ring behavior. When we analyzed the distribution of fluorescent Dam1 rings after disassembly of microtubules, we found an accumulation of rings at the ends of the microtubule, suggesting that the rings do not disassemble but slide back as the protofilaments peel away from the ends (Figure 7D).

We furthermore demonstrated that the Dam1 ring complex bundles microtubules in vitro. Lateral mobility of the rings could be important for "dynamic bundling" of microtubules in which rings on bundled microtubules of mixed polarity interact directly with each other. This would allow motors to slide these bundled microtubules against each other (Figure 7D, bottom) without disrupting anaphase spindle integrity.

The Role of a Ring at the Kinetochore

To explain how kinetochores can remain attached to growing and shortening microtubules, the existence of sleeves or collars into which the kinetochore microtubules insert have been hypothesized (Hill, 1985). The Dam1 ring complex could form such a sleeve in budding yeast. Moreover, our cryo-EM analysis, as well as the decoration of mixed lattice microtubules with fluorescent Dam1 complex, suggest that a GMPCPP lattice (which mimics the GTP or GDP-Pi bound state of the microtubule) is the preferred binding partner for the Dam1 ring complex. As one consequence, ring formation may be sensitive to the small structural changes in the lattice that accompany GTP hydrolysis or P_i release. Such a feature of the Dam1 complex would allow the kinetochore to recognize and preferentially bind to the microtubule plus end. Upon attachment of the kinetochore to the microtubule via the Dam1 ring complex, the microtubule plus end would be stabilized by the ring complex (Figure 7A). Similar to a proposal based on in vitro studies of kinetochore-microtubule interactions (Severin et al., 1997), GTP hydrolysis is expected to produce a lattice that is less favorable for Dam1 ring formation, and the kinetochore would therefore occupy the newly formed GTP cap by lateral diffusion or de novo ring assembly (Figure 7A).

In future studies, it will be important to analyze the dynamic behavior of the Dam1 ring complex on microtubules, the attachment of further kinetochore complexes to this binding interface, and the molecular details of the phospho regulation of this attachment by the Aurora-kinase Ipl1p. Furthermore, whether a similar ring complex is formed by the kinetochores of higher animals will be an important question for the future.

Insights into Organization and Functions of Dam1 Subunits

The biological functions and regulatory interactions of the Dam1 complex have been extensively studied by genetic analysis. Our biochemical and structural analyses of wt and mutant Dam 1 complexes have allowed us to analyze the contributions of specific subunits to complex function and to relate biological and biochemical activities. Mutations like *duo1-2* or *dam1Q185Stop* lead to the expression of a partially assembled complex consisting of Ask1p, Spc19p, Dad2p, Dad4p, and Hsk3p. This suggests that the *duo1-2* mutation could lead to a destabilization of the Dam1 complex at the restrictive temperature in vivo. Interestingly, three subunits of this partial complex, Ask1p, Spc19p, and Dad2p, are all acidic proteins (pI = 4.47, 4.59, and 3.97, respectively), and we demonstrated that they are unable to bind to microtubules, indicating that the microtubule binding module of the Dam1 complex is formed by the highly basic proteins Dam1p, Duo1p, and Spc34p (pI = 9.97, 10.76, and 8.6, respectively). This suggestion of subcomplexes within the Dam1 complex agrees well with results from two-hybrid and direct binding assays, which indicate that Dam1p, Duo1p, and Spc34p interact closely with each other (Ikeuchi et al., 2003; Shang et al., 2003).

Whereas the wt Dam1 complex bound strongly to microtubules with a dissociation constant of K_d = 0.2 μM, which is in the range determined for brain MAPs like tau (Goode and Feinstein, 1994), binding of the dam1-19 complex to microtubules was markedly reduced, implicating the C-terminal domain of Dam1p in establishing the contact to the microtubule. Importantly, *dam1* mutants that mimic or prevent Ipl1p phosphorylation of the complex showed regular subunit composition and wt microtubule binding activities. Thus, Aurora phosphorylation does not seem to destabilize or influence the microtubule binding activities of the complex. This is in agreement with the observation that *dam1* phosphomutants and *ipl1* ts mutants do not show gross spindle integrity phenotypes (Cheeseman et al., 2002a; Kang et al., 2001). An important future aim will be to map onto the ring structures the locations of the individual subunit proteins and the surfaces that are phosphorylated by Ipl1p and other kinases.

Experimental Procedures

Purification of Recombinant Dam1 Complex from Bacteria

To express recombinant Dam1 complex, plasmid pC43HSK3H (Miranda et al., 2005) was transformed into BL21Rosetta cells (Novagen) containing the pRARE plasmid. 2.5 l *Eschericia Coli* bacterial culture was grown at 37°C to OD 0.4, and protein expression was induced by the addition of 1 mM IPTG. Bacteria were harvested after 4 hr, washed in phosphate buffer saline (PBS), and resuspended in 20 mM sodium phosphate (pH 6.8), 500 mM NaCl, 1 mM EDTA, 20 mM Imidazol, and 0.5% (v/v) Triton X-100. Cells were lysed by sonication, and the lysate was cleared by centrifugation. The supernatant was incubated with Ni-NTA Agarose (Qiagen), equilibrated in PBS, and rotated for 2 hr at 4°C. Agarose beads were collected by low-speed centrifugation, washed twice, and resuspended in 6 ml 20 mM sodium phosphate, 500 mM NaCl, 1 mM EDTA, and 200 mM imidazole. After 2 hr rotation at 4°C, the supernatant was collected and dialyzed overnight against 20 mM sodium phosphate, 150 mM NaCl, and 1 mM EDTA. The dialysate was then loaded onto a 1 ml HiTrap SP sepharose cation exchange column (Amerham Pharmacia), and proteins were eluted by using a 10 ml linear gradient of 0.15 to 1 M NaCl in Buffer A. Dam1 complex was eluted at 600 mM NaCl. The corresponding fractions were collected, concentrated with a Centricon 30 (Amicon) device (preblocked with 2% BSA), and applied to a Superose 6 gel filtration column. The column was developed with 25 mM sodium phosphate (pH 6.8), 500 mM NaCl, and 1 mM EDTA. Dam1 containing fractions were snap frozen in liquid N_2 and stored at −80°C.

Mutations in *Dam1* and *Duo1* were introduced by Quikchange site-directed mutatgenesis on the pC43HSK3H expression plasmd (Stratagene). They were confirmed by DNA sequencing, and the mutant complexes were expressed and purified as described above.

Fluorescent Labeling of Dam1 Complex with Alexa-488

500 μl HiTrapS purified Dam1 complex (~500 μg) was incubated with 100 μM Alexa-488-C5-maleimide (Molecular Probes) for 1 hr at 0°C in the dark. The reaction was stopped by the addition of 1 mM DTT, and the sample was purified by gel filtration on a Superose 6 column (Amersham Pharmacia). The labeling stoichiometry was calculated from the absorption spectrum and found to be 1.9 mol dye/mole complex. Alexa-488 Dam1 complex was snap frozen in 50 μl aliquots and stored at −80°C. After thawing, the sample was kept at 4°C, as repeated freezing and thawing led to decreased fluorescence and degradation of the complex.

Microtubule Polymerization Assays

Tubulin polymerization was followed by right angle light scattering at 350 nm with a band pass of 1.78 nm in a Fluoromax-Spectrophotometer (Horiba). The absorption was recorded every 10 s for 1600 s. 70 μl polymerization reactions containing the indicated amounts of tubulin and Dam1 complex in 80 mM PIPES/KOH, (pH 6.8), 1 mM $MgCl_2$, and 1 mM EGTA (PEM) with 25% (v/v) glycerol were pipetted on ice and transferred to the prewarmed 37°C cuvette chamber. After the reaction, an aliquot was fixed by the addition of glutaraldehyde to 0.1% (v/v) and centrifuged onto coverslips as described (Evans et al., 1985). The coverslips were fixed for 3 min in methanol, rehydrated in PBS + 1 mg/ml BSA + 0.1% NP-40 (PBN) and incubated with Tub2.1-FITC conjugated anti-β-tubulin antibody (Sigma 1:50 in PBN) for 20 min at RT.

To follow dilution-induced disassembly, microtubules were assembled from 15 μM tubulin in the presence and absence of Dam1 complex. The polymerization reactions were diluted 1:1 by the addition of 70 μl warm PEM buffer, and disassembly was followed by light scattering. The reaction was transferred to TLA 100 tubes (Beckman) and centrifuged for 15 min at 60 K. Supernatant and pellet fractions were analyzed on a 12.5% SDS-PAGE.

Preparation of Segmented GMPCPP/GDP Microtubules

3 μM unlabeled tubulin was assembled with 100 μM GMPCPP (Jena Bioscience) in a 10 μl volume for 15 min at 37°C. To elongate these GMPCPP seeds, 10 μl of 50 μM tubulin (5:1 unlabeled tubulin:rhodamine tubulin) with 1 mM GTP was added and elongation was allowed to continue for 15 min. 2 μl of the segmented microtubule mix was incubated with 2 μl Alexa-488 Dam1 complex (dialyzed against 25 mM potassium phosphate [pH 6.8], 150 mM KCl, and 1 mM EDTA). Binding was allowed for 10 min, then 1 μl of the binding reaction was fixed with 1 μl 1% glutaraldehyde, 7 μl PEM, and 1 μl 10× Oxygen-Scavenging-Mix (1 × OSM:200 μg/ml glucose oxidase, 35 μg/ml catalase, 4.5 mg/ml glucose, and 0.5% β-mercaptoethanol). 2 μl of this mix was squashed under an 18 × 18 mm coverslip and viewed by fluorescence microscopy with a 60× Nikon objective on a Nikon Eclipse fluorescence microscope.

To visualize Alexa-labeled Dam1 complex on depolymerizing microtubules, 1.5 μl GMPCPP microtubules loaded with Alexa-Dam1 complex were incubated with 2 μl recombinant XKCM1 (residues 187–592, 0.3 μM), 1.5 μl 10 mM MgATP, 3 μl PEM, and 1 μl 10x OSM. The reactions were stopped by addition of 1 μl 1% glutaraldehyde.

Microtubule Binding Assays

Binding assays were performed essentially as described (Cheeseman et al., 2001a). Prior to binding, the Dam1 complex was dialyzed in Slide-A-Lyzer (Pierce) minidialysis units against 20 mM sodium phosphate (pH 6.8), 150 mM NaCl, and 1 mM EDTA. The dialysate was diluted with PEM buffer and centrifuged at 60,000 rpm for 15 min in a TL100 rotor to remove aggregates. Binding to taxol-stabilized microtubules was allowed for 10 min at RT. Microtubules were then sedimented by centrifugation at 25,000 rpm in a TL100 rotor for 20 min at RT.

EM

Electron microscopy of Dam1-decorated microtubules or self-assembled Dam1 complex, as well as cryo-EM of samples frozen in vitreous ice, was performed according to published protocols. Detailed descriptions of these procedures are available as Supplemental Data online.

Limited Proteolysis of Tubulin with Subtilisin

To remove the C terminus of both α- and β-tubulin, 15 μM taxol-stabilized microtubules were incubated with 40 μg/ml subtilisin in PEM buffer for 1 hr at 30°C. The reaction was stopped by the addition of 1 mM PMSF, the microtubules were pelleted by centrifugation (TLA100, 15 min, 60 K, and 25°C), washed twice, and resuspended in the original volume of PEM-buffer.

Acknowledgments

The authors wish to thank J.J. Miranda and Stephen Harrison for generously providing the Dam1 expression plasmid and Claire Walzcak for the kind gift of recombinant XMCAK1. The authors thank all members of the Barnes/Drubin Lab for discussions. This work was supported by grants from the National Institute of General Medical Sciences to G.B. (GM-47842), and E.N. (GM51487-09), the Office of Basic Energy Science of the US Department of Energy under contract DE-AC03-76F00098, and a postdoctoral fellowship of the Deutsche Forschungsgemeinschaft (DFG) to S.W. E.N. is a Howard Hughes Medical Institute Investigator. Research in this article was supported in part by a grant to D.G.D. from Philip Morris USA Inc. and Philip Morris International.

Received: December 2, 2004
Revised: December 29, 2004
Accepted: December 30, 2004
Published: January 20, 2005

References

Cheeseman, I.M., Enquist-Newman, M., Müller-Reichert, T., Drubin, D.G., and Barnes, G. (2001a). Mitotic spindle integrity and kinetochore function linked by the Duo1p/Dam1p complex. J. Cell Biol. *152*, 197–212.

Cheeseman, I.M., Brew, C., Wolyniak, M., Desai, A., Anderson, S., Muster, N., Yates, J.R., Huffaker, T.C., Drubin, D.G., and Barnes, G. (2001b). Implication of a novel multiprotein Dam1p complex in outer kinetochore function. J. Cell Biol. *155*, 1137–1146.

Cheeseman, I.M., Drubin, D.G., and Barnes, G. (2002a). Simple centromere, complex kinetochore: linking spindle microtubules and centromeric DNA in budding yeast. J. Cell Biol. *157*, 199–203.

Cheeseman, I.M., Anderson, S., Jwa, M., Green, E.M., Kang, J., Yates, J.R., 3rd, Chan, C.S., Drubin, D.G., and Barnes, G. (2002b). Phospho-regulation of kinetochore-microtubule attachments by the Aurora kinase Ipl1p. Cell *111*, 163–172.

De Wulf, P., McAinsh, A.D., and Sorger, P.K. (2003). Hierarchical assembly of the budding yeast kinetochore from multiple subcomplexes. Genes Dev. *17*, 2902–2921.

Desai, A., Verma, S., Mitchison, T.J., and Walczak, C.E. (1999). Kin I kinesins are microtubule-destabilizing enzymes. Cell *96*, 69–78.

Enquist-Newman, M., Cheeseman, I.M., Van Goor, D., Drubin, D.G., Meluh, P., and Barnes, G. (2001). Dad1p, third component of the Duo1p/Dam1p complex involved in kinetochore function and mitotic spindle integrity. Mol. Biol. Cell *12*, 2601–2613.

Evans, L., Mitchison, T., and Kirschner, M. (1985). Influence of the centrosome on the structure of nucleated microtubules. J. Cell Biol. *100*, 1185–1191.

Goode, B.L., and Feinstein, S.C. (1994). Identification of a novel microtubule binding and assembly domain in the developmentally regulated inter-repeat region of tau. J. Cell Biol. *124*, 769–782.

He, X., Rines, D.R., Espelin, C.W., and Sorger, P.K. (2001). Molecular analysis of kinetochore-microtubule attachment in budding yeast. Cell *106*, 195–206.

Hill, T.L. (1985). Theoretical problems related to the attachment of microtubules to kinetochores. Proc. Natl. Acad. Sci. USA *82*, 4404–4408.

Hinshaw, J.E., and Schmid, S.L. (1995). Dynamin self-assembles into rings suggesting a mechanism for coated vesicle budding. Nature *374*, 190–192.

Hofmann, C., Cheeseman, I.M., Goode, B.L., McDonald, K.L., Barnes, G., and Drubin, D.G. (1998). Saccharomyces cerevisiae

Duo1p and Dam1p, novel proteins involved in mitotic spindle function. J. Cell Biol. *143*, 1029–1040.

Hyman, A.A., Chretien, D., Arnal, I., and Wade, R.H. (1995). Structural changes accompanying GTP hydrolysis in microtubules: information from a slowly hydrolyzable analogue guanylyl-(alpha,beta)-methylene-diphosphonate. J. Cell Biol. *128*, 117–125.

Ikeuchi, A., Sasaki, Y., Kawarasaki, Y., and Yamane, T. (2003). Exhaustive identification of interaction domains using a high-throughput method based on two-hybrid screening and PCR-convergence: molecular dissection of a kinetochore subunit Spc34p. Nucleic Acids Res. *31*, 6953–6962.

Janke, C., Ortiz, J., Tanaka, T.U., Lechner, J., and Schiebel, E. (2002). Four new subunits of the Dam1-Duo1 complex reveal novel functions in sister kinetochore biorientation. EMBO J. *21*, 181–193.

Jones, M.H., Bachant, J.B., Castillo, A.R., Giddings, T.H., and Winey, M. (1999). Yeast Dam1p is required to maintain spindle integrity during mitosis and interacts with the Mps1p kinase. Mol. Biol. Cell *10*, 2377–2391.

Jones, M.H., He, X., Giddings, T.H., and Winey, M. (2001). Yeast Dam1p has a role at the kinetochore in assembly of the mitotic spindle. Proc. Natl. Acad. Sci. USA *98*, 13675–13680.

Kang, J.-s., Cheeseman, I.M., Kallstrom, G., Velmurugan, S., Barnes, G., and Chan, C.S.M. (2001). Functional cooperation of Dam1, Ipl1, and the inner centromere protein (INCENP)-related protein Sli15 during chromosome segregation. J. Cell Biol. *155*, 763–774.

Kosco, K.A., Pearson, C.G., Maddox, P.S., Wang, P.J., Adams, I.R., Salmon, E.D., Bloom, K., and Huffaker, T.C. (2001). Control of microtubule dynamics by Stu2p is essential for spindle orientation and metaphase chromosome alignment in yeast. Mol. Biol. Cell *12*, 2870–2880.

Li, Y., Bachant, J., Alcasabas, A.A., Wang, Y., Qin, J., and Elledge, S.J. (2002). The mitotic spindle is required for loading of the DASH complex onto the kinetochore. Genes Dev. *16*, 183–197.

Maiato, H., Deluca, J., Salmon, E.D., and Earnshaw, W.C. (2004). The dynamic kinetochore-microtubule interface. J. Cell Sci. *117*, 5461–5477.

McAinsh, A.D., Tytell, J.D., and Sorger, P.K. (2003). Structure, function, and regulation of budding yeast kinetochores. Annu. Rev. Cell Dev. Biol. *19*, 519–539.

Miranda. J.J.L., De Wulf, P., Sorger, P.K., and Harrison, S.C. (2005). The yeast DASH complex forms closed rings on microtubules. Nat. Struct. Mol. Biol., in press.

Nogales, E., Whittaker, M., Milligan, R.A., and Downing, K.H. (1999). High-resolution model of the microtubule. Cell *96*, 79–88.

Okada, Y., and Hirokawa, N. (2000). Mechanism of the single-headed processivity: diffusional anchoring between the K-loop of kinesin and the C terminus of tubulin. Proc. Natl. Acad. Sci. USA *97*, 640–645.

Pearson, C.G., Maddox, P.S., Zarzar, T.R., Salmon, E.D., and Bloom, K. (2003). Yeast kinetochores do not stabilize Stu2p-dependent spindle microtubule dynamics. Mol. Biol. Cell *14*, 4181–4195.

Pearson, C.G., Yeh, E., Gardner, M., Odde, D., Salmon, E.D., and Bloom, K. (2004). Stable kinetochore-microtubule attachment constrains centromere positioning in metaphase. Curr. Biol. *14*, 1962–1967.

Severin, F.F., Sorger, P.K., and Hyman, A.A. (1997). Kinetochores distinguish GTP from GDP forms of the microtubule lattice. Nature *388*, 888–891.

Shang, C., Hazbun, T.R., Cheeseman, I.M., Aranda, J., Fields, S., Drubin, D.G., and Barnes, G. (2003). Kinetochore protein interactions and their regulation by the Aurora kinase Ipl1p. Mol. Biol. Cell *14*, 3342–3355.

Shpetner, H.S., and Vallee, R.B. (1989). Identification of dynamin, a novel mechanochemical enzyme that mediates interactions between microtubules. Cell *59*, 421–432.

van Breugel, M., Drechsel, D., and Hyman, A. (2003). Stu2p, the budding yeast member of the conserved Dis1/XMAP215 family of microtubule-associated proteins is a plus end-binding microtubule destabilizer. J. Cell Biol. *161*, 359–369.

Westermann, S., Cheeseman, I.M., Anderson, S., Yates, J.R., 3rd, Drubin, D.G., and Barnes, G. (2003). Architecture of the budding yeast kinetochore reveals a conserved molecular core. J. Cell Biol. *163*, 215–222.

Wieland, G., Orthaus, S., Ohndorf, S., Diekmann, S., and Hemmerich, P. (2004). Functional complementation of human centromere protein A (CENP-A) by Cse4p from Saccharomyces cerevisiae. Mol. Cell. Biol. *24*, 6620–6630.

Zheng, Y., Wong, M.L., Alberts, B., and Mitchison, T. (1995). Nucleation of microtubule assembly by a gamma-tubulin-containing ring complex. Nature *378*, 578–583.